

Newtonian Noise Limit in Atom Interferometers for Gravitational Wave Detection

Flavio Vetrano, Andrea Viceré

Dipartimento di Scienze di Base e Fondamenti - DiSBeF, Università degli Studi di Urbino “Carlo Bo”, I-61029 Urbino, Italy

INFN, Sezione di Firenze, INFN, I-50019 Sesto Fiorentino, Italy

E-mail: flavio.vetrano@uniurb.it, andrea.vicere@uniurb.it

Abstract. In this work we study the influence of the newtonian noise on atom interferometers applied to the detection of gravitational waves, and we compute the resulting limits to the sensitivity in two different configurations: a single atom interferometer, or a pair of atom interferometers operated in a differential configuration. We find that for the instrumental configurations considered, and operating in the frequency range $[0.1 - 10]$ Hz, the limits would be comparable to those affecting large scale optical interferometers.

PACS numbers: 04.80.Nn, 95.55.Ym, 03.75.Dg, 37.25.+k

Submitted to: *Class. Quantum Grav.*

1. Introduction

The direct detection of Gravitational Waves is one of the most exciting challenges of current scientific research. The first generation of ground-based optical interferometric detectors, including Virgo [1] and GEO600 [3] in Europe, and the LIGO [2] interferometers in USA, achieved design sensitivity and carried out several science runs, which set interesting upper limits on several classes of astrophysical sources [4, 5, 6, 7]. The construction of a “second generation” of optical interferometers, Advanced LIGO [8] and Virgo [9], and the new Japanese detector KAGRA [10], is well underway; thanks to the implementation of several technical upgrades, the advanced detectors are expected to come on line with a sensitivity about ten times better than first generation instruments. In the meanwhile, the conceptual design of third generation detectors, like the Einstein Telescope [11, 12], has started. For all these optical ground based detectors the sensitivity in the low frequency band, below 10 Hz, is ultimately limited by the so called “gravity gradient”, or Newtonian Noise (NN) [13, 14], whose source is the direct coupling of the test masses with any mass-density change in the environment, especially of seismic or atmospheric origin. Atom interferometers (see [15] for a review) have been

proposed recently as GW detectors [16, 17, 18, 19, 20, 21], on the basis of previous general ideas [22]. The question arises then, if the “low frequency wall” due to NN is relevant also for these new proposed detectors. In this paper we consider only the NN of seismic origin and we carry out a detailed calculation of its contribution to the sensitivity curve of a simple atom interferometer both in the “single detector” configuration and in the “coupled differential” configuration. We anticipate our conclusions: the atom interferometers are subject to NN in a degree similar to optical interferometers, and therefore will require appropriate technical solutions to overcome this limit in the frequency band below 10Hz. The paper is organized as follows: in section 2 we consider a definite atom interferometer and we compute its response to a fluctuating gravity field; in section 3 we apply the formulas to the case of a single detector deriving the limits on sensitivity; finally in section 4 we consider two atom interferometers operated in differential configurations.

2. Newtonian noise of seismic origin in atom interferometers

In optical interferometric GW detectors the test masses are suspended mirrors: a pendular suspension is indeed the best approximation on Earth for a freely falling test mass. In atom interferometers instead the role of test masses is played by atoms in free fall, hence our intent is to determine the influence of the Newtonian coupling to an external, time-varying mass distribution, on freely falling masses. Some general considerations are possible: if the effect originates from seismic noise, it is driven by an external masses displacement field generally of the form $W(\omega) \sim \omega^{-2}$, mediated by a transfer function from the seism to the test masses motion behaving also as ω^{-2} [14, 23, 24], where ω is the angular frequency. Therefore the effect on test masses is expected to be of the form $\theta(\omega) \Gamma \omega^{-4}$, where $\theta(\omega)$ is a kind of reduced transfer function, depending on the “detection device”, Γ is a scale factor depending on the model of seismic waves (it is recognized that the role of main source is played by Rayleigh surface waves, especially the fundamental mode and few overtones [23, 24]). To derive the actual expression of $\theta(\omega)$ for NN in an atom interferometer, we use the ABCD formalism for matter waves, described elsewhere in detail [20, 25].

Assume that the Hamiltonian of the motion is at most quadratic in momentum and position operators

$$H = \sum_{n,r=1}^3 \left[\frac{1}{2M} p_n \beta_{nr}(t) q_r + \frac{1}{2} p_n \alpha_{nr}(t) q_r - \frac{1}{2} q_n \delta_{nr}(t) p_r + \right. \\ \left. - \frac{M}{2} q_n \gamma_{nr}(t) q_r + f_n(t) p_n - M g_n(t) q_n \right] \quad (1)$$

where $p_{n(r)}$ and $q_{n(r)}$ are vectors of momentum and position, respectively, whereas $\alpha, \beta, \gamma, \delta$ are suitable square matrices (note that $\delta = -\alpha^T$, with T indicates the transposed matrix), and M is the atom rest mass. Consider an atoms’ beam (a Gaussian packet under paraxial approximation [20, 25, 26, 27, 28]) which is divided and

recombined through a sequence of R light-field beam splitters, supplied by the same laser: from the first beam splitter to the last one (the output port) we may identify two paths, conventionally labeled s and i . By exploiting the ttt theorem [25] for the atoms/beam splitter interactions, and the mid-point property of Gaussian beams [29], the phase difference at the output port of the interferometer can be written as:

$$\Delta\phi = \sum_{j=1}^R \left[(k_{sj} - k_{ij}) \frac{q_{sj} + q_{ij}}{2} - (\omega_{sj} - \omega_{ij}) t_j + (\theta_{sj} + \theta_{ij}) \right] \quad (2)$$

where $k_{s(i)j}$ is the momentum transferred to the atoms by the j -th beam splitter along the s (i) arm, $\omega_{s(i)j}$ is the angular frequency of the laser beam and $\theta_{s(i)j}$ is the phase of the laser beam at the j -th interaction, $q_{s(i)j}$ is the distance of j -th interaction point from the laser source; equal masses are assumed for the atoms along the s and i paths. The expression in (2) is manifestly gauge-invariant [20, 25], and the evolution of the wave packets can be obtained, by means of the Ehrenfest theorem, from Hamilton's equations for the vector $\chi(t)$ [20, 25, 28]

$$\frac{d\chi}{dt} = \left(-\frac{\frac{dH}{dp}}{M \frac{dH}{dq}} \right) = \Gamma(t) \cdot \chi(t) + \Phi(t) \quad (3)$$

where

$$\chi \equiv \begin{pmatrix} q \\ \frac{p}{M} \end{pmatrix}; \quad \Phi(t) \equiv \begin{pmatrix} f(t) \\ g(t) \end{pmatrix}; \quad \Gamma(t) \equiv \begin{pmatrix} \alpha(t) & \beta(t) \\ \gamma(t) & \delta(t) \end{pmatrix} \quad (4)$$

in the form

$$\chi(t) = \begin{pmatrix} A(t, t_0) & B(t, t_0) \\ C(t, t_0) & D(t, t_0) \end{pmatrix} \cdot \left[\chi(t_0) + \begin{pmatrix} \xi(t, t_0) \\ \psi(t, t_0) \end{pmatrix} \right] \quad (5)$$

where

$$\begin{pmatrix} A(t, t_0) & B(t, t_0) \\ C(t, t_0) & D(t, t_0) \end{pmatrix} = \tau \exp \left[\int_{t_0}^t \Gamma(t') dt' \right], \quad (6)$$

$$\begin{pmatrix} \xi(t, t_0) \\ \psi(t, t_0) \end{pmatrix} = \int_{t_0}^t \begin{pmatrix} A(t_0, t') & B(t_0, t') \\ C(t_0, t') & D(t_0, t') \end{pmatrix} \cdot \Phi(t') dt'; \quad (7)$$

here τ represents the time-ordering operator, and an appropriate perturbative expansion can be used to evaluate the time-ordered exponential in (6) [20, 25, 28].

As a simple reference configuration let us consider a ‘‘Ramsey-Bord ’’ atom interferometer, with a Mach-Zender geometry, as outlined in figure 1 [15, 20, 25]. In the following, we will also assume that the instrument is crossed by a plane GW with ‘‘+’’ polarization and amplitude h , propagating along the $x_3 = z$ axis, perpendicular to the plane of the interferometer; we adopt in the following a description in Fermi coordinates, which represent the best approximation to the Laboratory Cartesian system [30].

Assuming the same ‘‘stable’’ frequency for the laser beams and neglecting the steady proper laser phases, the phase shift formula in (2) becomes

$$\Delta\phi = \sum_{j=1}^4 (k_{sj} - k_{ij}) \frac{q_{sj} + q_{ij}}{2}. \quad (8)$$

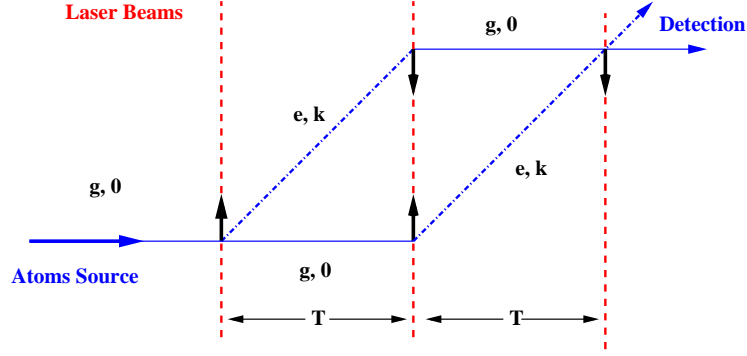


Figure 1. A simple atom interferometer with Mach-Zehnder geometry. Continuous horizontal lines, and the slanted dot-dashed lines, represent atom beams. Vertical dashed lines represent the laser beams; the bold continuous arrows represent relevant momentum transferred to the atoms; g and e mark the ground and excited internal states of the atoms; \mathbf{k} is the transverse momentum in \hbar units.

Let us assume that atoms are subjected only to a fluctuating gravitational field $g(t)$. Considering (1), (3), (4) and (7) we have

$$\begin{aligned} \alpha = \delta = \gamma = 0; \quad \beta = 1; \quad f(t) = 0; \quad g(t) \neq 0 \\ A = 1; \quad B = t - t_0; \quad C = 0; \quad D = 1; \end{aligned} \quad (9)$$

and we obtain

$$\begin{pmatrix} \xi(t, t_0) \\ \psi(t, t_0) \end{pmatrix} = \int_{t_0}^t \begin{pmatrix} t_0 - t' \\ t' \end{pmatrix} g(t') dt'. \quad (10)$$

We are interested in the low frequency range, where the newtonian noise is expected to be the limiting factor on account of its ω^{-4} shape. We will therefore assume that the single atom interferometer has a linear dimension smaller than the wavelength of seismic surface waves, which we will assume to set also the coherence length. Introducing the Fourier transform $\hat{g}(\omega)$ of the fluctuating field we can also write

$$\begin{aligned} \xi(t, t_0) &= \int \frac{d\omega}{2\pi} \hat{g}(\omega) \left[-\frac{(t-t_0)}{i\omega} e^{i\omega t} - \frac{1}{\omega^2} (e^{i\omega t} - e^{i\omega t_0}) \right] \\ \psi(t, t_0) &= \int \frac{d\omega}{2\pi} \hat{g}(\omega) \left[\frac{e^{i\omega t_0}}{i\omega} (e^{i\omega(t-t_0)} - 1) \right] \end{aligned} \quad (11)$$

and we assume, in the long wavelength approximation, that $\hat{g}(\omega)$ is the same at any point of the interferometer. Therefore the solution of the Hamilton equations (5) can be written as

$$\begin{aligned} \begin{pmatrix} q(t) \\ \frac{p(t)}{M} \end{pmatrix} &= \begin{pmatrix} 1 & t - t_0 \\ 0 & 1 \end{pmatrix} \cdot \left[\begin{pmatrix} q(t_0) \\ \frac{p(t_0)}{M} \end{pmatrix} + \right. \\ &\quad \left. \int \frac{d\omega}{2\pi} \hat{g}(\omega) \begin{pmatrix} -\frac{(t-t_0)}{i\omega} e^{i\omega t} - \frac{1}{\omega^2} (e^{i\omega t} - e^{i\omega t_0}) \\ \frac{e^{i\omega t_0}}{i\omega} (e^{i\omega(t-t_0)} - 1) \end{pmatrix} \right]; \end{aligned} \quad (12)$$

by iterating the relation in (5) to the four interaction points of the interferometer

in figure 1, setting $t_3 = t_2$ and defining $T = t_4 - t_3 = t_2 - t_1$, we finally obtain the phase shift at the output port of the interferometer:

$$\Delta\hat{\phi}(\omega) = kT^2 e^{i\omega T} \left[\frac{\sin(\omega T/2)}{(\omega T/2)} \right]^2 \hat{g}(\omega); \quad (13)$$

this is the fundamental formula to estimate the effect of the fluctuating field \hat{g} . We recall that k is the unperturbed wave vector of the laser beam, corresponding to the impulse (in units of the reduced Planck constant \hbar) transferred to the atom at each interaction point. Note also that in the limit $\omega \rightarrow 0$ the expression in (13) corresponds to the well known static result [29, 31].

3. Newtonian-Noise limit on sensitivity: the single detector case

In the weak field approximation, to first order in the amplitude h of an impinging gravitational wave, the phase shift at the output of the interferometer in figure 1 has been already obtained in a fully covariant way [20]. Indicating with q_1 the unperturbed distance of the first interaction point from the laser, and with p_1 the unperturbed momentum of the atoms, just before the first interaction with the laser beam, we recall that the Fourier transform of the phase shift, as a function of the Fourier transformed amplitude \hat{h} of the GW, can be written as

$$\begin{aligned} \Delta\hat{\phi}(\omega) = & \omega\hat{h}(\omega) \frac{T^2 k}{M} \left(p_1 + \frac{k\hbar}{2} \right) \times \left[\frac{e^{i\omega T} - e^{2i\omega T}}{\omega T} + i e^{i\omega T} \left(\frac{\sin(\omega T/2)}{\omega T/2} \right)^2 \right] + \\ & + \frac{\omega^2 \hat{h}(\omega)}{2} T^2 k q_1 \left(\frac{\sin(\omega T/2)}{\omega T/2} \right)^2 e^{i\omega T} \end{aligned} \quad (14)$$

in which the proper laser phases have been neglected. For a single interferometer with the laser source close to the device, the last term can be neglected and the more relevant one is the dynamic term, proportional to p_1 ; we can also neglect the recoil term $\frac{k\hbar}{2M}$. This expression can be directly translated into a relation between linear power spectral densities (LPSD), that we denote by a tilde, defined in terms of the two-point correlation functions as

$$\langle \hat{g}(\omega) \hat{g}(\omega') \rangle = 2\pi\delta(\omega - \omega') \tilde{g}^2(\omega) \quad (15)$$

in which the angular brackets represent the statistical average. From (13) and (14) we obtain

$$\begin{aligned} \Delta\tilde{\phi}(\omega) &= \tilde{h}(\omega) k L |\sin(\omega T/2)| \sqrt{1 - \frac{2\sin(\omega T)}{\omega T} + \left[\frac{\sin(\omega T/2)}{(\omega T/2)} \right]^2} \\ \Delta\tilde{\phi}(\omega) &= kT^2 \left[\frac{\sin(\omega T/2)}{(\omega T/2)} \right]^2 \tilde{g}(\omega) \end{aligned} \quad (16)$$

where the overall linear size $L = 2Tp_1/M$ of the interferometer in figure 1 has been introduced; combining the two equations, we deduce the expression

$$\tilde{h}_{NN}(\omega) = \frac{4}{\omega^2} \frac{|\sin(\omega T/2)|}{\sqrt{1 - \frac{2\sin(\omega T)}{\omega T} + \left[\frac{\sin(\omega T/2)}{(\omega T/2)} \right]^2}} \frac{\tilde{g}(\omega)}{L} \quad (17)$$

for the equivalent strain \tilde{h}_{NN} induced by the fluctuating field $\tilde{g}(\omega)$.

For definiteness, it is useful to discuss here the scale of the $\tilde{g}(\omega)$ LPSD, referring to typical values measured at the site of the Virgo interferometers; we recall indeed that we are considering the effect of an external fluctuating gravity field on freely falling test masses, which is the same situation experienced by the test masses of optical interferometers [14, 23, 24]; even though the detailed shape of the NN affecting a instrument like Virgo depends on the model for the seismic sources and the superficial Earth layers, similar results are obtained in different cases, which can be summarized as follows

$$\tilde{h}_{NN}(\omega) = \frac{\sqrt{4}\tilde{X}(\omega)}{L_V} \simeq \frac{1.2 \times 10^{-9}}{\omega^2} \tilde{x}_{seism}(\omega) \times \frac{Hz^2}{m} \quad (18)$$

where $L_V = 3000\text{m}$ is the length of Virgo arms, $\tilde{X}(\omega)$ is the displacement LPSD for a single suspended mirror, and $\tilde{x}_{seism}(\omega)$ is the measured LPSD of the ground seism [32]; the factor $\sqrt{4}$ takes into account that in Virgo the noise due to the four end-station mirrors adds in quadrature. Considering the relation between the mirror motion and its acceleration, due to the fluctuating gravitational field, $\tilde{g}(\omega) = \omega^2 \tilde{X}(\omega)$, we obtain

$$\frac{\tilde{g}(\omega)}{L} = \frac{\omega^2 L_V}{2L} \frac{\sqrt{4}\tilde{X}(\omega)}{L_V} \simeq 6 \times 10^{-10} \frac{L_V}{L} \tilde{x}_{seism}(\omega) \times \frac{Hz^2}{\text{m}}; \quad (19)$$

we further assume that the seismic noise measured at the Virgo site is well approximated by [33]

$$\tilde{x}_{seism}(\omega) \simeq \frac{10^{-7}}{[\omega / (2\pi\text{Hz})]^2} \text{m Hz}^{-1/2}; \quad (20)$$

assuming an atom interferometer with $L \sim 200\text{m}$, we obtain

$$\frac{\tilde{g}(\omega)}{L} \sim \frac{10^{-16}}{[\omega / (2\pi\text{Hz})]^2} \text{Hz}^2. \quad (21)$$

We show in figure 2 examples of the newtonian noise of (17) assuming the expression in (21) for the LPSD of the fluctuating gravitational field, and setting $T = 0.4\text{ s}$ for the time of flight of the atoms between the interaction points in the interferometer.

The zeroes represent frequencies at which the atom interferometer is insensitive both to the gravity gradient noise and to GW.

4. Two detectors operated in a differential configuration

Let us now consider the second term in (14), proportional to the position q_1 . This term, already introduced in a different context [34], is a sort of “clock” term which takes into account the influence of the GW on the laser beam, along its path from the source to a well defined physical point. Its role was discussed in recent papers [35, 36, 37] and the most relevant new property is the introduction of q_1 (path of laser beam) in place of L (path of atom beam); so, in order to improve the sensitivity, enlarging q_1 seems in principle easier than enlarging L ; however, the need of measuring the distance from the laser, and strong requirements about coherence and stability while maintaining

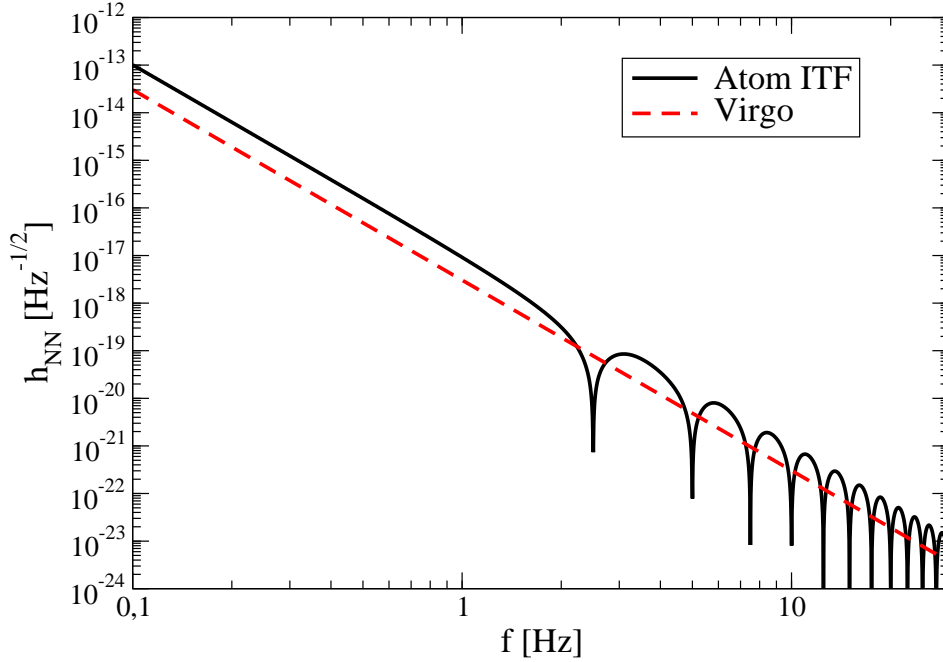


Figure 2. The solid curve represents the effect of the gravity gradient noise on a single atom interferometer, with the expected ω^{-4} behaviour and zeroes corresponding to frequencies at which the instrument is insensitive both to the gravity gradient fluctuations and to gravitational waves. For comparison, the dashed curve represents the model NN effect on the Virgo interferometer.

sufficient power density for the laser beam, are not minor issues, which prevent drawing too optimistic conclusions about the practicality of the configuration. Anyway the suggestion of adopting a two-interferometers differential configuration [21] appears very appealing in order to overcome the first of the mentioned problems; furthermore it may yield a good common-modes rejection. Under the hypothesis of a common laser source for two identical Mach-Zehnder atom interferometers in differential configuration, for which the relative distance D satisfies the condition $\omega D/c \ll 1$ (with c the speed of light in vacuum), from (14) the overall difference between the two partial phase differences at the output ports can be formally obtained as

$$\Delta\hat{\phi}(\omega) = 2k D \sin^2(\omega T/2) e^{i\omega T} \hat{h}(\omega) \quad (22)$$

where $D \equiv q_1^I - q_1^I$ as anticipated. Considering also (13) we obtain for the differential configuration

$$\hat{h}_{NN}(\omega) = \frac{2}{\omega^2 D} [\hat{g}_2(\omega) - \hat{g}_1(\omega)], \quad (23)$$

where the difference in the right hand side requires some discussion. In a given frequency band, if the two fluctuating gravity fields $\hat{g}_{1,2}$ act upon sufficiently distant interferometers, they will be uncorrelated, and we will obtain for the LPSD simply a sum in quadrature

$$\tilde{h}_{NN}(\omega) = \frac{2}{\omega^2 D} \sqrt{\tilde{g}_1^2(\omega) + \tilde{g}_2^2(\omega)} \quad (24)$$

displaying no conceptual difference with respect to the limits obtained for optical interferometers with long D arms [32]. Considering instead a low-frequency, long-wavelength approximation, it may be appealing the situation in which, even with two separated interferometers, the residual correlation leads to a partial noise cancellation in (23).

We recall that the signals $\hat{g}_{1,2}(\omega)$ are assumed to be stochastic acceleration fields in positions 1 and 2, projected along the direction specified by the segment \vec{D} as in figure 3

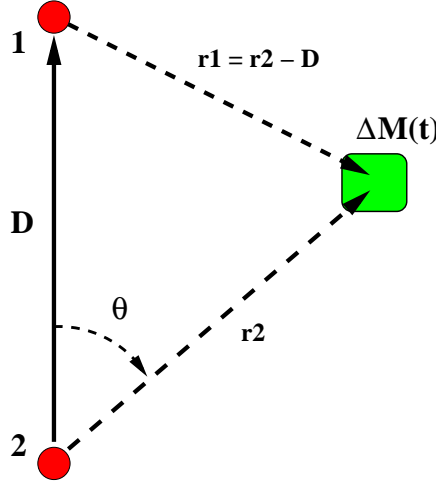


Figure 3. Geometry of the detector: atom interferometers are located at positions 1 and 2, and a fluctuating mass element is assumed at a location \vec{r}_2 in a frame having position 2 as the origin, and a \hat{z} axis parallel to \vec{D} .

We further assume to model the stochastic noise in the simplest possible way, namely as due to uncorrelated fluctuations in the density of the material surrounding the detector [14]. In other words a density fluctuation $\Delta M(t)$ will contribute to the acceleration field in points 1 and 2 as

$$\vec{g}_2(t) = \frac{G\Delta M(t)}{r_2^2} \hat{r}_2 = \frac{G\Delta M(t)}{r_2^3} \vec{r}_2 \quad (25)$$

$$\vec{g}_1(t) = \frac{G\Delta M(t)}{r_1^2} \hat{r}_1 = \frac{G\Delta M(t)}{|\vec{r}_2 - \vec{D}|^3} (\vec{r}_2 - \vec{D}) \quad (26)$$

Considering only the component acting along the direction separating the two points 1 and 2, we obtain

$$\begin{aligned} g_2(t) &= \frac{G\Delta M(t)}{r^2} \cos(\theta) \\ g_1(t) &= \frac{G\Delta M(t)}{[r^2 + D^2 - 2rD \cos(\theta)]^{3/2}} [r \cos(\theta) - D] \end{aligned} \quad (27)$$

as the contribution to the fluctuation of the acceleration field due to a single mass element. To obtain the total fluctuation, we need now to sum over the space.

We first assume that the space can be considered homogeneous around the detectors: this is the case for instance if the instruments are placed in a deep mine,

at a depth much larger than D . We are therefore interested in the quantity

$$\begin{aligned}\hat{h}_{NN}(\omega, \vec{r}) &= \frac{2}{\omega^2 D} [\hat{g}_2(\omega) - \hat{g}_1(\omega)] \\ &= \frac{2G\Delta M(\omega, \vec{r})}{\omega^2 D} \left\{ \frac{\cos(\theta)}{r^2} - \frac{r \cos(\theta) - D}{[r^2 + D^2 - 2rD \cos(\theta)]^{3/2}} \right\}\end{aligned}\quad (28)$$

which should be summed over the volume. It is convenient to evaluate the spectral density

$$\begin{aligned}\langle h_{NN}(\omega) h_{NN}(\omega') \rangle &\equiv 2\pi\delta(\omega - \omega') \tilde{h}_{NN}^2(\omega) \\ &= \sum_{\vec{r}, \vec{r}'} \left\langle \Delta h_{NN}(\omega, \vec{r}) \Delta h_{NN}(\omega', \vec{r}') \right\rangle;\end{aligned}\quad (29)$$

where, following again Saulson [14], we assume the sum to be extended over volume elements of linear size $\lambda/2$, with ΔM fluctuating coherently inside these regions, and totally uncorrelated otherwise:

$$\langle \Delta M(\omega, \vec{r}) \Delta M(\omega', \vec{r}') \rangle = 2\pi\delta(\omega - \omega') \Delta \tilde{M}^2(\omega, \vec{r}) \delta_{\vec{r}, \vec{r}'}.\quad (30)$$

We obtain therefore

$$\tilde{h}_{NN}^2(\omega) = \frac{4G^2}{\omega^4 D^2} \sum_{\vec{r}} \Delta \tilde{M}^2(\omega, \vec{r}) \left\{ \frac{\cos(\theta)}{r^2} - \frac{r \cos(\theta) - D}{[r^2 + D^2 - 2rD \cos(\theta)]^{3/2}} \right\}^2.\quad (31)$$

If we additionally assume that the mass fluctuations do not depend on \vec{r} , we can further simplify, obtaining

$$\begin{aligned}\tilde{h}_{NN}^2(\omega) &= \frac{4G^2 \Delta \tilde{M}^2(\omega)}{\omega^4 D^2} \sum_{\vec{r}} \left\{ \frac{\cos(\theta)}{r^2} - \frac{r \cos(\theta) - D}{[r^2 + D^2 - 2rD \cos(\theta)]^{3/2}} \right\}^2 \\ &= \frac{4G^2 \Delta \tilde{M}^2(\omega)}{\omega^4 D^2} \left(\frac{2}{\lambda} \right)^3 \int \left\{ \frac{\cos(\theta)}{r^2} - \frac{r \cos(\theta) - D}{[r^2 + D^2 - 2rD \cos(\theta)]^{3/2}} \right\}^2 r^2 dr d\cos\theta d\phi,\end{aligned}\quad (32)$$

where we have approximated the sum with an integral, normalizing by the volume element of the coherent region $(\lambda/2)^3$. If we were to retain only the first term, we would obtain the same result as in [14], corrected for a factor 2. The integration over the angular functions is directly carried out, resulting in a lengthy expression:

$$\begin{aligned}\tilde{h}_{NN}^2(\omega) &= \frac{64\pi G^2 \Delta \tilde{M}^2(\omega)}{\omega^4 D^2 \lambda^3} \cdot H(D, \lambda) \\ H &= \int \frac{r \left\{ 4[8(D-r)^2(D+r)^2 + 3Dr(3D^2 - r^2)] - 3(D^2 - r^2)^2 \ln \frac{(D-r)^2}{(D+r)^2} \right\}}{24D^3(D-r)^2(D+r)^2} dr + \\ &+ \int \frac{2(D^3 + 2r^3)(D-r)}{3D^3 r^2 |D-r|} dr\end{aligned}\quad (33)$$

which, as expected, displays double poles in $r = 0$ and in $r = D$. Both divergences are artefacts, which should be regulated introducing cutoffs $r \geq \frac{\lambda}{4}$ and at $|r - D| \geq \frac{\lambda}{4}$. However, it is now necessary to distinguish two cases

Short wavelength If the distance $D \gg \lambda$, then the integral over r gives

$$H(D, \lambda) = \frac{14}{3\lambda} + O\left(\frac{\lambda}{D^2} \ln \frac{\lambda}{D}\right) \quad (34)$$

and we obtain

$$\tilde{h}_{NN(sw)}^2(\omega) \simeq \frac{896 \pi G^2 \Delta \tilde{M}^2(\omega)}{3 \omega^4 D^2 \lambda^4}. \quad (35)$$

Long wavelength In the long wavelength approximation the integral in (33) can be carried out assuming $r \geq \frac{\lambda}{4} \gg D$, obtaining

$$H(D, \lambda) = \frac{512 D^2}{15 \lambda^3} + O\left(\frac{D^4}{\lambda^5}\right) \quad (36)$$

hence

$$\tilde{h}_{NN(lw)}^2(\omega) \simeq \frac{32768 \pi G^2 \Delta \tilde{M}^2(\omega)}{15 \omega^4 \lambda^6}; \quad (37)$$

it seems at first surprising that the dependence on D in this case cancels out, whereas one could have expected to retain a dependence, which could lead to zero noise in the $D \rightarrow 0$ limit case. However, we are actually in a situation in which the instrument is sensitive to the gradient of the gravity acceleration (see (23)), and therefore, barring other sources of noise, the sensitivity is independent on the baseline D .

We can now use Eq.12 of [24] to relate the mass fluctuations with the measured seism

$$\Delta \tilde{M}^2(\omega) = \frac{1}{16} \lambda^6 \rho_0^2 \left(\frac{\pi}{\lambda}\right)^2 \tilde{x}_{seism}^2(\omega) \quad (38)$$

where ρ_0 is the density of the medium. We finally obtain

$$\tilde{h}_{NN(sw)}(\omega) \simeq \frac{2\pi\sqrt{14\pi}G\rho_0}{\sqrt{3}\omega^2 D} \tilde{x}_{seism}(\omega) \quad (39)$$

$$\tilde{h}_{NN(lw)}(\omega) \simeq \frac{16\sqrt{2\pi}G\rho_0}{\sqrt{15}\omega c_L} \tilde{x}_{seism}(\omega) \quad (40)$$

where we have used the relation $\lambda\omega = 2\pi c_L$, with c_L the speed of longitudinal seismic waves; typically in the ground where Virgo is installed $c_L \simeq 1000 \text{ m s}^{-1}$, whereas we can assume $\rho_0 \simeq 2.7 \times 10^3 \text{ kg m}^{-3}$ as a typical value for the continental crust. Assuming $D \simeq 200 \text{ m}$, we obtain

$$\tilde{h}_{NN(sw)}(\omega) \simeq \frac{2 \times 10^{-8}}{\omega^2} \tilde{x}_{seism}(\omega) \times \frac{\text{Hz}^2}{\text{m}} \quad \frac{\omega}{2\pi} \gg \frac{c_L}{D} \simeq 5 \text{ Hz} \quad (41)$$

$$\tilde{h}_{NN(lw)}(\omega) \simeq \frac{2 \times 10^{-9}}{\omega} \tilde{x}_{seism}(\omega) \times \frac{\text{Hz}}{\text{m}} \quad \frac{\omega}{2\pi} \ll \frac{c_L}{4D} \simeq 1 \text{ Hz} \quad (42)$$

Comparing with (18) for the gravity gradient noise affecting the Virgo interferometer, we see that in the short wavelength limit, represented by (41), the frequency dependence (as expected) is the same. Instead, in the long wavelength limit (42), the NN affecting the

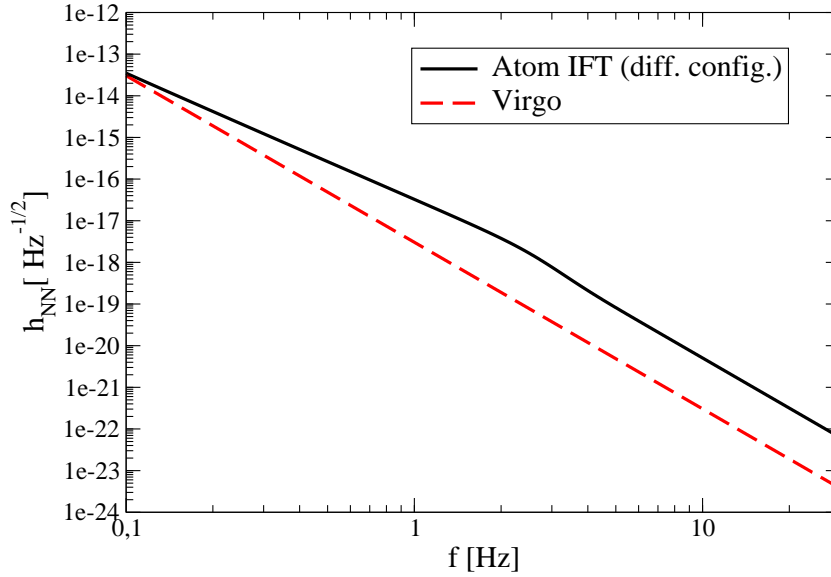


Figure 4. Comparison of models of the Newtonian Noise as seen by the Virgo interferometer (dashed line) or by an hypothetical pair of atom interferometers operated in differential configuration (continuous line). Above a few Hz, the different scale of the two curves reflects the different baseline of the two instruments: 3km for the length of Virgo arms, 200m for the distance between the atom interferometers.

atom interferometer has a slower growth for $\omega \rightarrow 0$, reflecting the presence of correlated noise at the two stations, that partially cancels out in (23).

The NN limit to the atom interferometer sensitivity is displayed in figure 4, over a frequency range which runs from the long to the short wavelength regimes, assuming as reference the same seismic noise \tilde{x}_{seism} as in (20). We display for comparison also the NN affecting the Virgo instrument; in the high frequency regime, the pair of atom interferometers behaves like a smaller Virgo, at a scale about one order of magnitude larger because of the shorter baseline; in the low frequency regime is evident the milder growth as $\omega \rightarrow 0$, insufficient though to push the noise below the limit affecting Virgo, unless the frequency range is extended well below 10^{-1}Hz .

5. Conclusions

In this work we have evaluated the effect of fluctuations of the gravity field on the sensitivity of atom interferometers, thus providing an estimate of the so-called newtonian (or gravity gradient) noise for this kind of instruments. We have seen that a mid-scale atom interferometer, with a baseline $L \sim 200\text{m}$, is subject to a noise essentially equivalent to the one affecting a large scale optical interferometer, as Virgo. We have also found that operating two small-scale atom interferometers, placed at a similar distance $D \sim 200\text{ m}$, in differential configuration, the level of g.g. noise is generally larger, by at most an order of magnitude in the frequency range considered.

We conclude that, similarly to what is foreseen for future optical interferome-

ters [11], operating successfully atom interferometers in the [0.1, 10] Hz frequency window will require to mitigate the gravity gradient noise, either by choosing very quiet, possibly underground sites, or by devising clever noise subtraction strategies.

We acknowledge that this study has a limitation in the model for the gravity fluctuations, which is approximate; however, as it has been the case for similar studies carried out for optical interferometers [24, 23], we believe that the use of more refined models will change the numerical results only by small factors, which would not alter our conclusions.

Bibliography

- [1] Accadia A et al. (Virgo Collaboration) 2012 *JINST* **7** P03012
- [2] Abbott B et al. 2009 *Rep. Prog. Phys.* **72** 076901
- [3] <http://www.geo600.org>
- [4] Abadie J et al. (LIGO Scientific Collaboration and Virgo Collaboration) 2012, *Phys. Rev. D* **85** 082002
- [5] Abadie J et al. (LIGO Scientific Collaboration and Virgo Collaboration) 2012 *ApJ* **760** 12
- [6] Abadie J et al. (LIGO Scientific Collaboration and Virgo Collaboration) 2011 *ApJ* **737** 93
- [7] Abbott B P et al. (LIGO Scientific Collaboration and Virgo Collaboration) 2009 *Nature* **460** 990
- [8] Harry G M et al. (LIGO Scientific Collaboration) 2010 *Class. Quantum Grav.* **27** 084006
- [9] <https://wwwcascina.virgo.infn.it/advirgo>
- [10] <http://gwcenter.icrr.u-tokyo.ac.jp/en/>
- [11] Punturo M et al. 2010 *Class. Quantum Grav.* **27** 194002
- [12] Sathyaprakash B et al. 2012 *Class. Quantum Grav.* **29** 124013
- [13] Spero R 1983 in *Science Underground*, Los Alamos Conf. 1982, AIP Conf. Proceedings, N.Y.
- [14] Saulson P 1983 *Phys. Rev. D* **30** 732-736
- [15] Berman P (Ed) 1997 *Atom Interferometry*, N.Y., Academic Press
- [16] Vetrano F, in *2004 Aspen Winter Conference on GW and their Detection*, http://www.ligo.caltech.edu/LIGO_web/Aspen2004/pdf/vetrano.pdf
- [17] Chiao R Y and Spiliotopoulos A D 2004 *J. Mod. Optics* **51** 861
- [18] Roura A, Brill D R, Hu B L, Misner C W and Phillips W D 2006 *Phys. Rev. D* **73** 084018
- [19] Delva P, Angonin M C and Tournenc P 2006 *Phys. Lett. A* **357** 249
- [20] Tino G M and Vetrano F 2007 *Class. Quantum Grav.* **24** 2167
- [21] Dimopoulos S, Graham P W, Hogan J M, Kasevich M and Rajendran S 2008, *Phys. Rev. D* **78** 122002
- [22] Bordé C J 1989 *Phys. Lett. A* **140** 10-12
- [23] Hughes S A and Thorne K S 1998 *Phys. Rev. D*, **58** 122002/1-30
- [24] Beccaria M et al. 1998 *Class. Quantum Grav.* **15** 3339-3362
- [25] C.J. Bordé 2004 *Gen. Rel. Grav.* **36** 475
- [26] J.F. Riou, Y. Le Coq, F. Impens, W. Guerin, C.J. Bordé, A. Aspect and P. Bouyer 2008 *Phys. Rev. A* **77** 033630
- [27] Bordé C J 2008 *Eur. Phys. J.* **163**, 315 (2008)
- [28] Tino G M and Vetrano F 2011 *Gen. Rel. Grav.* **43** 2037
- [29] Bordé C J 2002 *Metrologia* **39** 435-463
- [30] Manasse F K and Misner C W 1963 *J. Math. Phys.* **4** 735
- [31] Bordé C J 2001 C. R. Acad. Sci. Paris, t2 - Ser. IV 509-530
- [32] AA.VV. 1999 *The Virgo sensitivity curve*, VIR-NOT-PER-1390-51, <https://wwwcascina.virgo.infn.it/senscurve/VIR-NOT-PER-1390-51.pdf>
- [33] Accadia T et al. (Virgo Collaboration) 2011 *Low Frequency Noise and Active Control* **30** 63-79

- [34] Bordé C J, Sharma J, Tourenç P and Damour T 1983 *J. Physique Lett.* **44** L983
- [35] Müller H, Chiow S, Hermann S and Chu S 2009 *Phys. Rev. Lett.* **102** 240403
- [36] Hoensee M, Lan S, Houtz R, Chan C, Estey B, Kim G, Kuan P and Müller H 2011 *Gen. Rel. Grav.* **43** 1905
- [37] Hogan J M, Johnson D M S, Dickerson S, Kovachy T, Sugarbaker A, Chiow S, Graham P W, Kasevich M, Saif B, Rajendran S, Bouyer P, Seery B D, Feinberg L and Keski-Kuha R 2011 *Gen. Rel. Grav.* **43** 1953